

## New Early Pleistocene Perissodactyl remains associated with *Gigantopithecus* from Yanliang Cave, Guangxi of southern China

Yaling Yan<sup>a,b</sup>, Yuan Wang<sup>a\*</sup>, Min Zhu<sup>a</sup>, Shaokun Chen<sup>a,b,c</sup>, Dagong Qin<sup>d</sup> and Changzhu Jin<sup>a</sup>

<sup>a</sup>Key Laboratory of Vertebrate Evolution and Human Origins, Institute of Vertebrate Paleontology and Paleoanthropology, Chinese Academy of Science, Xi-Zhi-Men-Wai Street 142, Beijing 100044, P.R. China; <sup>b</sup>University of Chinese Academy of Science, Beijing 100049, P.R. China; <sup>c</sup>Chongqing Thress Gorges Institute of Paleoanthropology, China Three Gorges Museum, Chongqing 400015, P.R. China; <sup>d</sup>School of Life Sciences, Peking University, Beijing 100871, P.R. China

(Received 4 February 2015; accepted 10 March 2015)

Herein the new Perissodactyl fossils associated with *Gigantopithecus blacki* recovered from Yanliang Cave, Guangxi of southern China were described as *Hesperotherium sinense*, *Tapirus sanyuanensis* and *Rhinoceros fusuiensis*, which are all the common elements of the typical Early Pleistocene *Gigantopithecus*–*Sinomastodon* fauna in southern China. Especially, we analyse and compare to the metacarpus and metatarsus among extinct *Rhinoceros fusuiensis* and extant Asian rhinos based on quantitative indexes of measurements. The results show that the sizes between genera *Rhinoceros* and *Dicerorhinus* are different. Specifically, the sizes of metacarpus and metatarsus of *Rhinoceros fusuiensis* are smaller than those of the living *Rhinoceros* (*Rhinoceros unicornis* and *Rhinoceros sondaicus*), but greater than those of *Dicerorhinus sumatrensis*. So, the measurements of metacarpus and metatarsus can be considered to provide available evidence in identifying rhino fossils. The assemblage of Perissodactyl remains from Yanliang Cave is most similar to those of Longgupo Cave, Chongqing and Mohui Cave, Guangxi, indicating its age as the early Early Pleistocene (~2.0 Ma). These Perissodactyl fossils also implied a tropical bushy and forested environment with the humid and warm climate favourable for habitation of high-evolved primates such as *Gigantopithecus blacki*.

**Keywords:** Perissodactyla; *Rhinoceros fusuiensis*; *Gigantopithecus blacki*; Early Pleistocene; Yanliang Cave; Southern China

### Introduction

The *Gigantopithecus* faunal complex has been considered as one of the most important Quaternary mammalian faunas in East Asia. During the past decade, the most diverse and intriguing of the *Gigantopithecus* faunas have been discovered in the Chongzuo, Zuojiang River area, Guangxi Zhuang Autonomous Region (which is abbreviated to Guangxi ZAR) of southern China. The Pleistocene karst caves in Chongzuo, along Chinese and Vietnamese border, have unearthed interesting finds of the high-evolved primates *Gigantopithecus blacki* and *Homo sapiens* as well as a diverse associated vertebrate fauna (Jin, Pan, et al. 2009; Jin, Qin, et al. 2009; Liu et al. 2010; Jin et al. 2014; Zhang et al. 2014).

The vertebrate fossils have received the most detailed attention due to the taxonomic analyses of primates (Zhao et al. 2008; Zhang et al. 2010, 2014; Harrison et al. 2014; Takai et al. 2014), carnivores (Zhu et al. 2014, 2015), proboscideans (Wang, Jin, et al. 2014), artiodactyls (Dong et al. 2011, 2013, 2014), rhinos (Yan, Jin, et al. 2014; Yan, Wang, et al. 2014), small mammals (Jin et al. 2008, 2010; Wang et al. 2009, 2010) and lizards (Mead et al. 2014).

The Chongzuo cave sites including *Gigantopithecus blacki* and *Homo sapiens* have been dated by palaeomagnetic or U-series radio isotopic analyses from the Early to Late

Pleistocene with age-range estimates from approximately 2.0 Ma to 111 ka. Specifically, these sites include the following of Baikong Cave (2.0 Ma), Juyuan Cave (1.8 Ma), Sanhe Cave (1.2 Ma), Queque Cave (1.0 Ma), Hejiang Cave (400–320 ka) and Zhiren Cave (111 ka) (Jin, Qin, et al. 2009; Jin, Pan, et al. 2009; Liu et al. 2010; Jin et al. 2014; Sun et al. 2014; Zhang et al. 2014). These new discoveries from the Chongzuo sites, and their subsequent analysis, are providing a better understanding of the evolution of the *Gigantopithecus* fauna. Recently, there has been a new *Gigantopithecus* fauna *in situ* discovered in Yanliang Cave, Fusui County, Chongzuo City. The carnivore fossils from this cave were studied by Zhu et al. (2014, 2015) and the dental remains of rhinos were also described by Yan, Wang, et al. (2014) and Yan, Jin, et al. (2014).

Yanliang Cave (22°13'54"N, 107°36'35"E) is located on Gaoyan Mountain, Fusui County, Chongzuo City, Guangxi ZAR and about 100 km southwest of Nanning City (Figure 1). This cave, about 18 m long and 10 m wide (Figure 2(B)), was discovered in 2010 by a joint research team by Chinese Academy of Sciences and Peking University. The landscape of Chongzuo and its adjacent areas are characterised by a spectacular geomorphology of karst peaks developed under a northern tropical climate. As a consequence of the continuous uplift of this area since

\*Corresponding author. Email: [xiaowangyuan@ivpp.ac.cn](mailto:xiaowangyuan@ivpp.ac.cn)



Figure 1. (Colour online) Map showing the geographical location of YCF and other fossil sites. 1, Yanliang Cave (YCF); 2, Tianzhen (TS); 3, Huangjiawan (HZ); 4, Liucheng *Gigantopithecus* Cave (LGC); 5, Longgudong Cave (LCJ); 6, Longgupo Cave (LCW); 7, Renzidong Cave (RCF); 8, Yanjinggou (YC); 9, Guanyin Cave (GCQ); 10, Baikong Cave (BCL); 11, Mohui Cave (MCT); 12, Baeryan Cave (BCB); 13, Heizhai Quarry (HQH).

the beginning of Quaternary, multiple horizons of karst caves with different elevations have been developed. With the entrance 200 m above sea level (Figure 2(A)), Yanliang Cave roughly lies in the fifth horizon of the Chongzuo karst cave system, which corresponds with the *Gigantopithecus*-bearing Early Pleistocene sediments (Jin, Qin, et al. 2009; Jin, Pan, et al. 2009; Jin et al. 2014). The stratigraphic sequence in Yanliang Cave can be divided into four layers from top to bottom with a total thickness of approximately 6.8 m (Figure 2(C)). Abundant Perissodactyl remains reported here were recovered from the third layer composed of silty clay with calcareous breccias.

During the excavation in 2011, there were more than 40 mammalian taxa recovered from Yanliang Cave. Based on the faunal analysis, the geological age of Yanliang fauna is estimated to be the early Early Pleistocene (Yan, Wang, et al. 2014; Zhu et al. 2014, 2015), most similar to Baikong fauna (~2.0 Ma) in the same area (Jin et al. 2014; Sun et al. 2014). The present study provides the detailed taxonomic analyses of new Perissodactyl remains recovered from Yanliang Cave during the excavations in 2011, including three genera, *Hesperotherium*, *Tapirus* and *Rhinoceros*.

## Materials and methods

The Perissodactyl specimens described here are all archived in the fossil collection of Institute of Vertebrate Paleontology and Paleoanthropology, Chinese Academy of Science, Beijing, China. Measurements (mm) are made with a digital caliper for teeth and bones. For the dental terminology, we follow Owen (1870), Coombs (1978), Qiu (2002) and Tong (2006) on *Hesperotherium*, and Owen (1870) and Tong (2005) on *Tapirus*. The terminology and measurements used here for *Rhinoceros* are modified from Guérin (1980) and Qiu and Wang (2007).

The abbreviations of localities and institute are listed as follows: BCB, Baeryan Cave, Bijie City, Guizhou Province; BCL, Baikong Cave, Liyu Mountain, Chongzuo, Guangxi ZAR; GCQ, Guanyin Cave, Qianxi County, Guizhou Province; HQH, Heizhai Quarry, Hezhang County, Guizhou Province; HZ, Huangjiawan, Zhen'an County, Shaanxi Province; LGC, Liucheng *Gigantopithecus* Cave, Guangxi ZAR; LCJ, Longgudong Cave, Jianshi County, Hubei Province; LCW, Longgupo Cave, Wushan County, Chongqing City (formerly Sichuan Province);

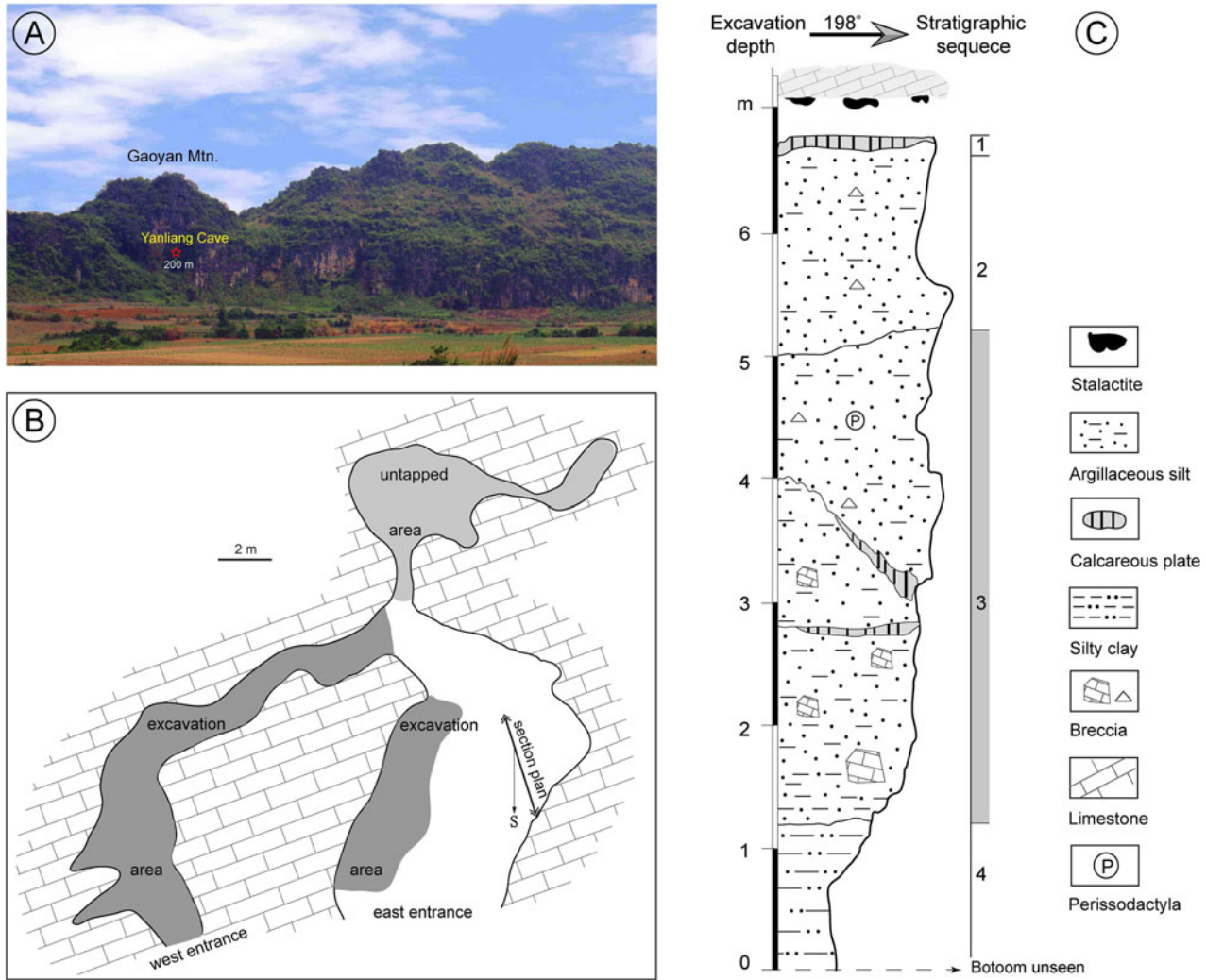


Figure 2. (Colour online) Map showing geomorphological landscape (A), plan (B) and stratigraphic sequence (C) of Yanliang Cave.

MCT, Mohui Cave, Tiandong County, Guangxi ZAR; RCF, Renzidong Cave, Fangchang County, Anhui Province; TS, Tianzhen County, Shanxi Province; YC, Yanjinggou (= Yenchingkou), Chongqing City (formerly Sichuan Province); YCF, Yanliang Cave, Fusui County, Guangxi ZAR; IVPP (V), Institute of Vertebrate Paleontology and Paleoanthropology, Chinese Academy of Science.

**Systematic palaeontology and comparisons**

*Chalicothere*

- Family Chalicotheriidae Gill, 1872
- Subfamily Chalicotheriinae Gill, 1872
- Genus *Hesperotherium* Qiu, 2002
- Hesperotherium sinense* (Owen, 1870)

(Figure 3)

*New material and description*

One left m3 (V20158). This is a complete lower molar with slight wear. The length and width are, respectively, 37.5 and 22.1 mm, and the proportion of width/length is 58.9%. The crown is typically W-shaped, and the trigonid and talonid are V-shaped. The anterior part is slightly narrower than the posterior one. The position of paraconid is low, and the protoconid and hypoconid are equally high. The metaconid and entoconid are well developed. The paralophid is parallel to metalophid, and the protolophid is parallel to hypolophid. The anterior valley is shallower than the posterior valley. The external syncline is deep. The anterior cingulum is weak, and the well-developed posterior cingulum is positioned around the posterior edge of the tooth and extends obliquely from the lingual side downwards to buccal side. Both of the lingual and buccal cingula are missing.

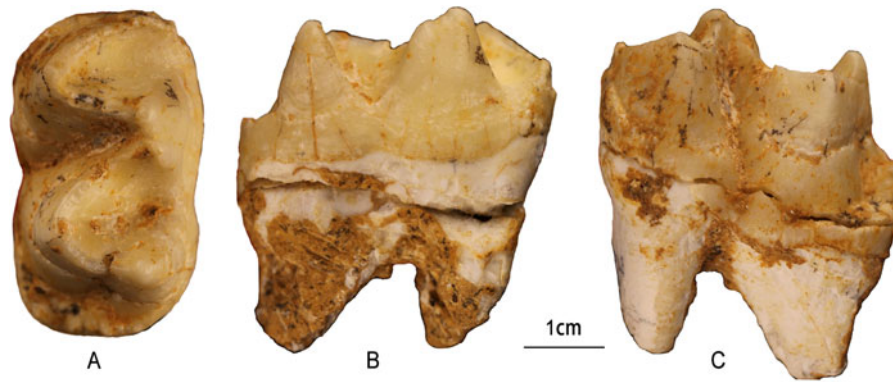


Figure 3. (Colour online) The left m3 (V20158) of *Hesperotherium sinensis* from Yanliang Cave. (A) Occlusal view, (B) lingual view and (C) labial view.

#### Comparison and comments

The developed posterior cingulum indicates that the YCF specimen differs from *Nestoritherium sivalense*. With brachyodont, well-developed posterior cingulum, proportionally larger and wider crown, and slightly larger size, the m3 from YCF can be assigned to the genus *Hesperotherium* established by Qiu (2002). There are two species of *Hesperotherium*: *Hesperotherium sinense* (Owen 1870) and *Hesperotherium huaiheense* (Jin and Liu 2009). Most of the Pleistocene *Hesperotherium* fossils from southern China have been assigned to *Hesperotherium sinense*, while *Hesperotherium huaiheense* only includes the specimens from RCF. The m3's length (46.5 mm) and width (26 mm) of *Hesperotherium huaiheense* are significantly greater than those of the YCF specimens. However, the size of YCF m3 is smaller than that of *Hesperotherium sinense* from TS, YC and HZ (Owen 1870; Colbert and Hooijer 1953; Qiu 2002; Li and Deng 2003), but the proportion of width/length of YCF m3 is inversely greater than that of the above three sites. Furthermore, the sizes of YCF m3 all fall within the range of the m3 length (36.5–40.2 mm), width (19.5–23.5 mm) and the proportion of width/length (56.4–58%) of *Hesperotherium sinense* from LGC. On dental morphology, the m3 from YCF and LGC are also similar to each other on the degree of development of anterior and posterior valleys and posterior cingulum (Tong, 2006). Thus, the YCF specimen can be assigned to *Hesperotherium sinense* and mostly resembles LGC specimens.

#### Tapir

Family Tapiridae Burnett, 1830

Genus *Tapirus* Brünnich, 1772

*Tapirus sanyuanensis* Huang and Fang, 1991

(Figure 4)

#### New materials

One DP4 (V20159.1), one I2 (V20159.2), one P1 (V20159.3), one P2 (V20159.4), two P3 (V20159.5–6), one P4 (V20159.7), one M1 (V20159.8), one M3 (V20159.9), two dp4 (V20159.10–11), one lower canine (V20159.12), two m2 (V20159.13–14), one metalophid of m2 (V20159.15), one m3 (V20159.16) and one metalophid of m3 (V20159.17).

#### Measurements

Tables 1 and 2.

#### Description

**Deciduous dentition.** DP4 ( $n = 1$ ). The crown is nearly trapezoid. The ectoloph and metaloph are weak, and the protocone and hypocone are well developed. Both the parastyle and anterior cingulum are present.

dp4 ( $n = 2$ ). The occlusal outline of the crown is approximately rectangular, and its anterior width is slightly larger than the posterior one. The metalophid is almost parallel to entolophid. The metaconid and entoconid in lingual side are equally developed with the protoconid and hypoconid in buccal side. The paralophid has diminished into a cingulum, together with anterior cingulum to form the double-cingula. The spiny secondary structure is present in the median valley. The posterior cingulum is weak. There are two tooth roots.

**Permanent dentition.** I2 ( $n = 1$ ). There is a developed lingual tubercle.

P1 ( $n = 1$ ). The outline of crown is sub-triangular, and posterior part is wider than anterior one. The ectoloph is distinct, and the parastyle is weak. The prominent paracone and metaloph are close to each other. The protocone is weak, and the hypocone is absent. The lingual

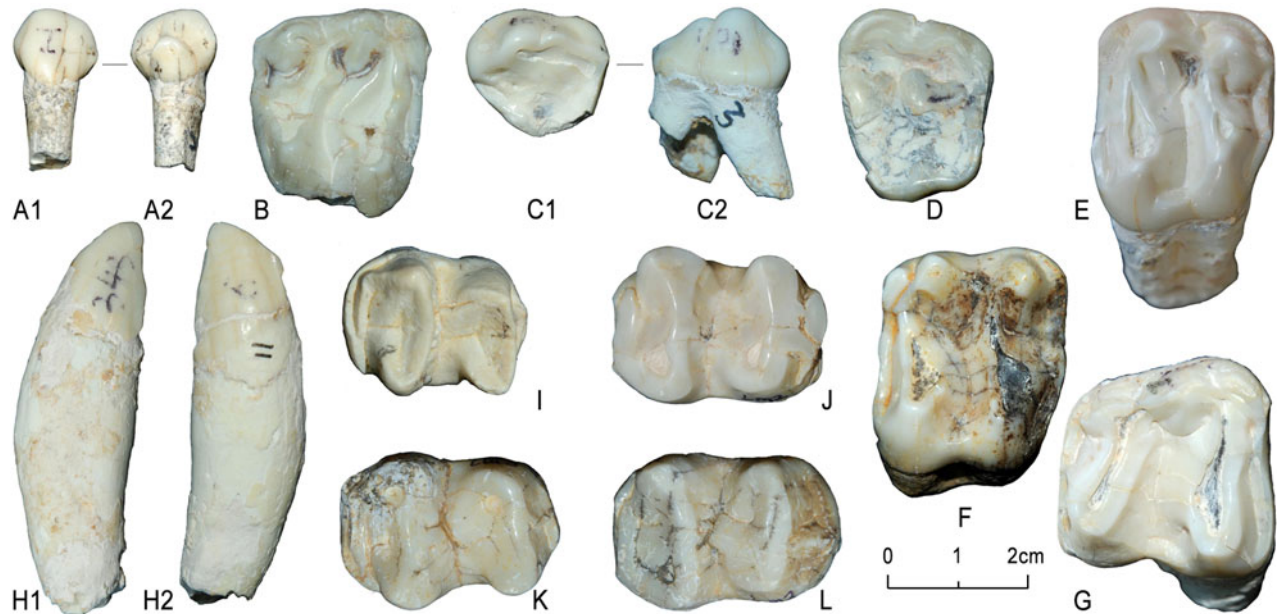


Figure 4. (Colour online) *Tapirus sanyuanensis* from Yanliang Cave. A, left I2 (V20159.2); B, right DP4 (V20159.1); C, left P1 (V20159.3); D, right P2 (V20159.4); E, left P3 (V20159.5); F, left P4 (V20159.7); G, right M3 (V20159.9); H, left canine (V20159.12); I, right dp4 (V20159.10); J, left m2 (V20159.14); K, right m2 (V20159.13); L, left m3 (V20159.16). A1 and C2, labial view; A2, lingual view; B, C1, D–G and I–L: occlusal view; H1, mesial view; H2, distal view.

cingulum is developed and connected to the posterior cingulum. Two tooth roots are present.

P2 ( $n = 1$ ). The crown outline is trapezoid with heavy wear. The enamel is thin with clear wrinkles. The ectoloph is developed and connected to the protoloph and metaloph. The metastyle is distinct and the postfossette can be obviously observed.

P3 ( $n = 2$ ). The crown is rectangular in occlusal outline and width is greater than length. The protoloph is slightly longer than metaloph. The ectoloph and parastyle are developed. The protocone and hypocone are more developed than paracone and metacone, between which there is a clear groove. The postfossette can be obviously observed. The metaloph slightly extends to the posterior side. The prominent anterior and posterior cingula both extend to the buccal side. The former ends at the base of parastyle, and the latter terminates on the base of the groove of ectoloph.

P4 ( $n = 1$ ). The crown outline and basic dental morphology resemble those of P3. Compared to P3, the P4 has a larger length and a less width, more developed parastyle, anterior and posterior cingula, wider median valley, more posteriorly inclined metaloph and more prominent postfossette.

M1 ( $n = 1$ ) and M3 ( $n = 1$ ). Compared with upper premolars, the crown of M1 is quadrilateral in occlusal outline and width is greater than length. The ectoloph is short, protoloph and metaloph are obviously posteriorly inclined, and postfossette is not distinct. The anterior

cingulum is present without extending to buccal or lingual sides. The posterior cingulum is missing and the protoloph is more inflated than metaloph. The dental characters of M3 are similar to those of M1, while the differences are summarised as more degraded metaloph, wider median valley and more developed posterior cingulum.

Lower teeth ( $n = 8$ ). The lower canine is very developed, and the root is more robust than crown. The abrasive surface is on the front side. The permanent lower molars are similar to deciduous lower teeth on dental morphology while the differences are listed as a larger size, thicker and smoother enamel, more prominent double-cingula formed by paralophid and anterior cingulum, missing spiny secondary structure in the median valley and wider posterior cingulum.

#### Comparison and comments

The Pleistocene tapir fossils in southern China include three species: *Tapirus sanyuanensis*, *Tapirus sinensis* and *Megatapirus augustus*. The *Megatapirus augustus* is different from the YCF specimens on being an obvious larger size. The *Tapirus sinensis* is distinguished from other species by its median size, less proportion of width/length, distinct lingual cusps on P1, a developed buccal cingulum on upper teeth, and prominent anterior and posterior cingula (Owen 1870; Tong et al. 2002; Zheng 2004; Tong 2005). The YCF specimens differ from those of *Tapirus sinensis* from LCJ in bearing smaller sizes, a

Table 1. Metrical comparison of size ranges of upper teeth of *Tapirus sanyuanensis* from YCF and other Quaternary tapir fossils from southern China (mm)

	<i>Tapirus sanyuanensis</i>				<i>Tapirus sinensis</i>		<i>Megatapirus augustus</i>		<i>Tapirus indicus</i>
	YCF	LCW <sup>a</sup>	RCF <sup>b</sup>	LCJ <sup>c</sup>	LCJ <sup>c</sup>	Koken (1885)	YC <sup>d</sup>	Hooijer (1947)	
DP1	L W		20–21.5 (21) 18.5	21–24 (22) 18–21 (20)	19 17.5	26–27 (26.5) 22–24 (23) 30–32 (31)	19–22 14–21 23–25		
DP2	Wa Wp			25 25		27–28 (27.5) 30–31 (30.7)	19–22 22–25		
DP3	L Wa Wp		23.5 27 24.5	28 16 20		31–33 (32) 31–32 (31.5) 30	24–25 23–26 21–24		
DP4	L Wa Wp		25 >27	26 28		33–35 (34) 36–37 (36.5)	23–26 25–27		
P1	L W	18.5–19.6 (19.05) 16–18 (17)	18.5 16	20 16	19 17.5	25–29 (27.3) 22–26 (23.9)	19–22 14–21		
P2	L Wa Wp	19.5–20.5 (20) 24–24.5 (24.2) 20–21.8 (20.9)	22–23 (22.5) 22.5–23.5 (23) 25.5–27.5 (26.5)	24 22 27	21–22 (21.5)	27–32 (29.7) 28–35 (30.4) 32–40 (34.9)	22–24 17–23 24–27		
P3	L Wa Wp	23.7–23.8 (23.75) 29.8–34.1 (31.95) 28–31.6 (29.8)	22.3 26.9 22.6	24 29.5 30	22.5–25 (24.2) 21.5–23.5 (22.4) 22–28.5 (26.5)	29–31 (30.4) 36–41 (37.6) 36–42 (37.9)	22–25 26–29 26–28		
P4	L Wa Wp	20.8–24.1 (22.26) 26.5–33 (29.16) 25–30.1 (27.82)	22.5 32 30	19 19	26 30.5	29–33 (30.8) 38–40 (39.3) 36–39 (38)	22–23 28–31 26–29		
M1	L Wa Wp	21.9–25 (23.45) 27.1–31 (28.89) 25.2–30.1 (27.79)	25–26 (26) 29–32 (30) 25–27 (26)	28 32 27	21 25.5	32–35 (33.7) 37–43 (39.1) 32–37 (34.3)	24–27 24–28 22–25		
M2	L Wa Wp	25.5–28.8 (26.65) 28.8–35 (31.08) 24.8–32 (26.98)	27 34.5 29.5	32 36 30	24–26 (25) 25.5–29.5 (27.5)	34–38 (36.5) 39–46 (42.4) 36–40 (37.8)	25–28 29–31 24–28		
M3	L Wa Wp	25–30.5 (27.82) 28.2–33.6 (31.13) 23.5–28 (25.56)	29.5–30 (30) 31.5–33 (32) 26.5–27 (27)	31–33 (32) 34–37 (36) 28–30 (29)	24 29.5	34–38 (35.8) 39–41 (40.2) 31–33 (31.8)	24–28 27–30 23–25		

L, length; W, width; Wa, width of anterior lobe; Wp, width of posterior lobe.

<sup>a</sup>Huang and Fang (1991).<sup>b</sup>Jin and Liu (2009).<sup>c</sup>Zheng (2004).<sup>d</sup>Colbert and Hooijer (1953).

Table 2. Metrical comparison of size ranges of lower teeth of *Tapirus sanyuanensis* from YCF and other Quaternary tapir fossils from southern China (mm).

		<i>Tapirus sanyuanensis</i>				<i>Tapirus sinensis</i>		<i>Megatapirus augustus</i>	<i>Tapirus indicus</i>
		YCF	LCW <sup>a</sup>	RCF <sup>b</sup>	LCJ <sup>c</sup>	LCJ <sup>c</sup>	Koken (1885)	YC <sup>d</sup>	Hooijer (1947)
dp2	L			29		29		39–41 (39.7)	27–32
	W			16		17		21–23 (21.7)	13–16
dp3	L			23.5		25		31–33 (32.3)	23–26
	Wa			9.5		16.5		20–21 (20.3)	15–16
	Wp			16		17		21–22 (21.7)	14–17
dp4	L	26		24–25.5 (25)		26		33–35 (34.3)	24–27
	Wa	17–18.1 (17.55)		16.5–17 (17)		18		22–23 (22.7)	16–18
	Wp	16.8–17.4 (17.1)		17		17		23–24 (23.3)	15–18
p2	L		24.9–26.5 (25.72)	25–26 (26)			22.5–24 (23.3)	33–36 (34.3)	25–28
	W		14.8–17.1 (15.72)	15.5–16 (16)			13–15 (14)	20–22 (20.3)	13–17
p3	L		20.5–23.4 (21.83)	23		25	22.5–24 (23.25)	29–33 (30.8)	23–27
	Wa		15.1–16 (15.67)	16.5–18 (17)		17	16–20 (18.1)	21–23 (22)	15–18
	Wp		16.5–17.6 (17.03)	19		22		23–25 (23.9)	17–20
p4	L		24.1–26.5 (24.9)	23	26	26		30–32 (31.4)	23–25
	Wa		16.2–18.2 (17.25)	20	20	20.5		24–26 (25)	18–20
	Wp		18.1–19.2 (18.4)	19.5	20	23.5		24–26 (25.1)	19–22
m1	L		24.2–26.9 (25.73)	25–27 (26)	26	27	25	32–34 (33.5)	24–27
	Wa		17.2–18.5 (17.9)	18–20 (19)	20	22	19	24–26 (25.1)	17–20
	Wp		15–18.1 (16.23)	17–18.5 (18)	19.5	22		23–26 (23.8)	17–19
m2	L	30–30.2 (30.1)	27.2–29.9 (28.76)	29–30 (29.5)	26.5	32	30	35–39 (36.6)	26–28
	Wa	19–21.8 (20.67)	19–21 (20.11)	20–21 (20.5)	21	23	20–21 (20.5)	26–29 (27.3)	20–22
	Wp	17.3–18.4 (17.85)	17–18.5 (17.83)	18–20 (19)	20.5	24.5		25–26 (25.4)	18–21
m3	L	31.2	28–31.1 (29.68)	30	28			38–40 (38.4)	24–29
	Wa	22–22.7 (22.35)	19.1–21.2 (20.28)	22	20.5			27–29 (28)	19–21
	Wp	20.1	16.5–18.5 (17.34)	19	19			24–25 (24.2)	18–19

Notes: L, length; W, width; Wa, width of anterior lobe; Wp, width of posterior lobe.

<sup>a</sup>Huang and Fang (1991).

<sup>b</sup>Jin and Liu (2009).

<sup>c</sup>Zheng (2004).

<sup>d</sup>Colbert and Hooijer (1953).

less compressed parastyle and more reduced cingula. Moreover, YCF specimens resemble those of *Tapirus sanyuanensis* from LCW and RCF on the similar sizes, diminished lingual cups on P1, distinct parastyle and the similar degree of development of cingula on upper teeth. Thus, it is suitable to assign YCF specimens to *Tapirus sanyuanensis* based both on size and dental morphology.

### Rhino

Family Rhinocerotidae Owen, 1845

Subfamily Rhinocertinae Owen, 1845

Genus *Rhinoceros* Linnaeus, 1758

*Rhinoceros fusuiensis* Yan, Wang, Jin and Mead, 2014

(Figures 5 and 6)

### New materials

Three m2s (V18642.140–141, 147), three lower jaw fragments (V18642.148–150), one metacarpal III (V18642.151), five sesamoids (V18642.152–156), two

cuneiforms (V18642.157–158), one trapezoid (V18642.161), three unciforms (V18642.162–164), one metacarpal II (V18642.165), two metacarpal IVs (V18642.166–167), one PhI of middle digit (V18642.177), three PhIIs of middle digit (V18642.168–170), two PhIIIs of middle digit (V18642.171–172), four PhIs of lateral digit (V18642.173–176), one calcaneus (V18642.178), two metatarsus IIs (V18642.179–180) and two metatarsus IVs (V18642.181–182).

### Amended diagnosis

A relatively small body size with sub-hypsodont and the upper molars have the smaller proportion of width/length than other species of *Rhinoceros*. The i2 is robust. The paracone rib and metacone rib are weak on P2, but prominent on P3 and P4. The paracone rib is present and the metacone rib is degenerated or missed on upper molars. The crochets are moderately to strongly developed. The well-developed crochet is not connected to the protoloph, so the medifossette is absent. The

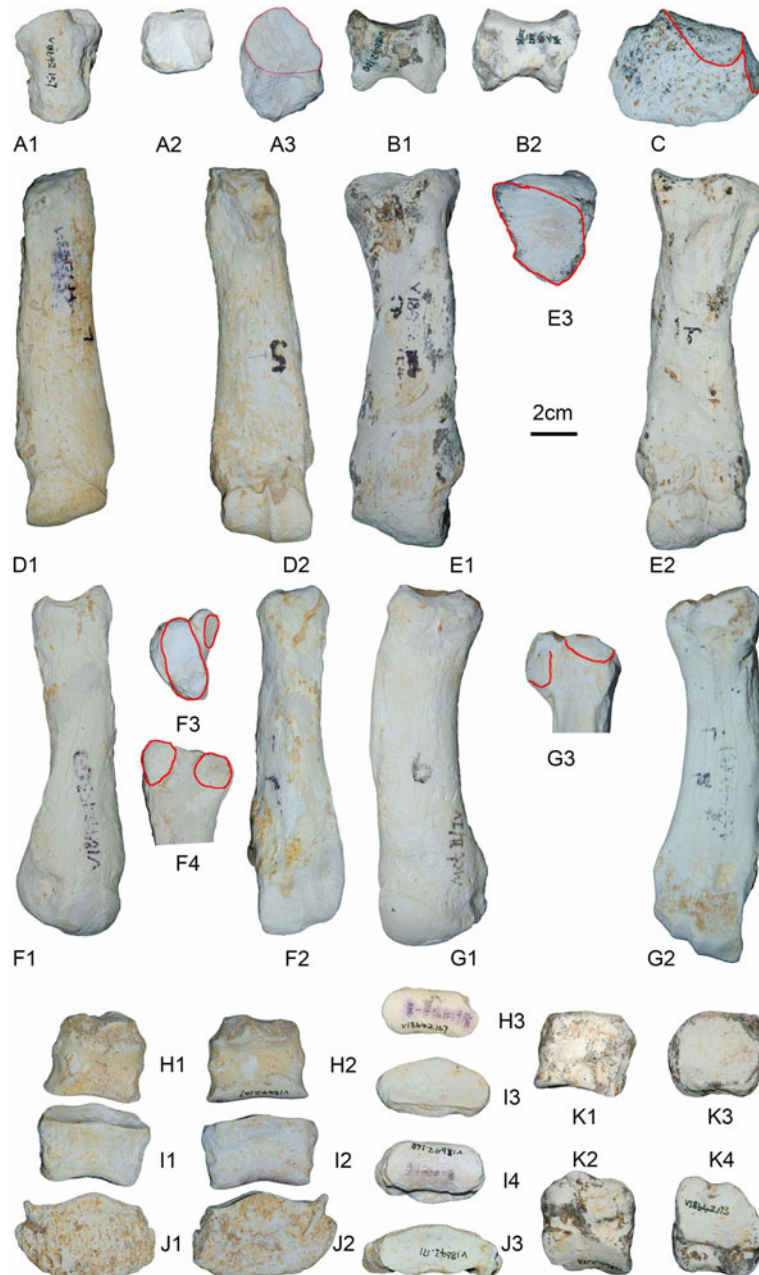


Figure 5. (Colour online) The postcranial remains of *Rhinoceros fusuiensis* from Yanliang Cave. A, right cuneiform (V18642.157); B, right trapezoid (V18642.161); C, right unciform (V18642.162), palmar view; D, right Mc II (V18642.165); E, right Mc IV (V18642.166); F, left Mt II (V18642.180); G, left Mt IV (V18642.182); H, Ph I of middle digit (V18642.177); I, Ph II of middle digit (V18642.168); J, Ph III of middle digit (V18642.171); K, Ph I of second/fourth finger (V18642.173). A1, dorsal view; D1–K1, palmar view; D2–K2, volar view; A2, E3–F3 and H3–K3, proximal view; A3, I4 and K4, distal view; B1, F4 and G3, mesial view; B2, lateral view.

crochet and ectoloph form a sharp angle. The antecrochet is absent. Both parastyle and metastyle are present. The protocone constriction is weak. Both of the anterior and posterior cingula are developed on the upper dentition. The crown of M3, without metacone rib, is triangular in occlusal outline. The length of the ectometaloph is longer than its height on the unworn M3. The size of metacarpals and metatarsals is close to that of

*Rhinoceros sondaicus*, and obviously greater than that of *Dicerorhinus sumatrensis*. The calcaneus is relatively small. The medial process of the calcaneal tuberosity is slightly inflated. The sustentacular facet and bone shaft form an obtuse angle, and the inflation degree of sustentacular facet is weaker than that formed on *Rhinoceros sondaicus*, *Rhinoceros unicornis* and *Rhinoceros sinensis*.



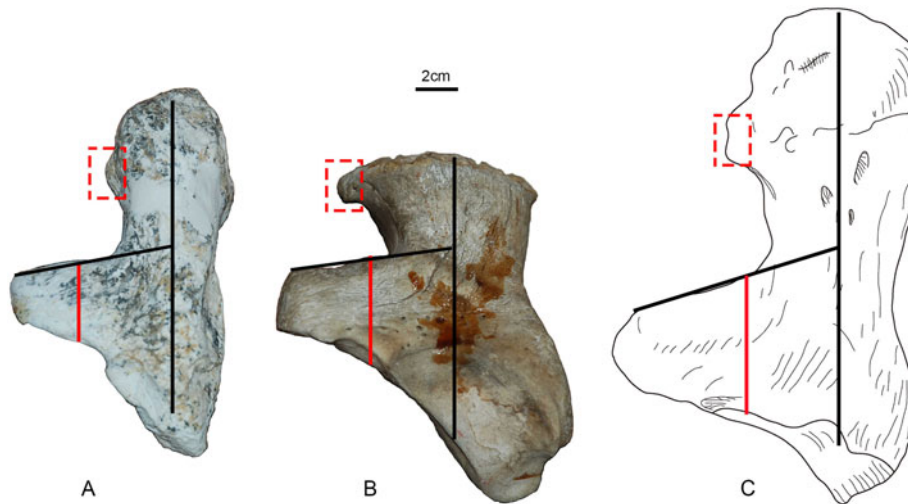


Figure 6. (Colour online) Metrical and morphological comparison of calcaneus among *Rhinoceros fusuiensis* from Yanliang Cave (A) and the extant Southeast Asian rhinos (B: *Rhinoceros unicornis* IVPP OV 1046; C: *Rhinoceros sondaicus* data from Guérin (1980)).

Measurements

Tables 3–5.

Description

*Fragments of lower jaw.* The teeth on the lower jaw fragments are well preserved but heavily worn. The dental morphology is very similar to that in Yan, Wang, et al. (2014).

*Carpals.* Cuneiform ( $n = 2$ ). One specimen (V18642.157) is relatively complete, and the other (V18642.158) only retains the articular facet connecting to the unciform. The outline of cuneiform is nearly trapezoidal in the dorsal view, and height is greater than width. In the proximal

view, the main articular facet linking to the ulna is saddle shaped. The articular facet connecting the pisiform is large. The articular facet attaching to the lunar is half-moon shaped. In the distal view, the articular facet in connection with unciform is circular in shape. The height is 40 mm, the width is 44 mm and the thickness is 44 mm in the dorsal view.

Trapezoid ( $n = 1$ ). Most of the articular facets are preserved. The articular facet with scaphoid is saddle shaped and strongly inclined to the external side in proximal view. The articular facet connecting the Mc II is quadrangular in the distal view. In the lateral view, the articular facet linking magnum is relatively flat. In the medial view, the height is 36 mm, the length is 29 mm and the thickness is 42 mm.

Table 3. Metrical data of MCs and Mts of *Rhinoceros fusuiensis* from YCF (mm).

	L	DT prox.	DAT prox.	DT dist.	DT artic. dist.	DAT artic. dist.	DAT dist.	DT dia.	DAT dia.
Mc II									
V18642.165	150+	36.2		43	35.5	38	26	35	20
Mc III									
V18642.151				54.5	46	37.2	36.6	46.7	21.7
Mc IV									
V18642.167	155	43.3	40	45	41			37	20
V18642.166	153	49	40.6	48	40.8	35.5	30	37	22
Mt II									
V18642.180	137	26	38	38.7	31	36	28.5	27	21
V18642.179	146+			39.7	33	32.1	25.5	31	22
Mt IV									
V18642.182	143	36.7	37.4	40	35.2	31	27.7	33	30
V18642.181	141	38.3	36	30	33.6	37.5	29	30	25

Notes: L, total length; DT prox., maximum transverse diameter of the proximal epiphysis; DAT prox., anterior–posterior diameter of the proximal epiphysis; DT artic. dist., maximum transverse diameter of the distal articulation; DAT artic. dist., anterior–posterior diameter of the distal articulation; DT dist., maximum transverse diameter of the distal epiphysis; DAT dist., anterior–posterior diameter of the distal epiphysis; DT dia., maximum transverse diameter of the shaft at its middle part; DAT dia., anterior–posterior diameter of the shaft at its middle part.

Unciform ( $n = 3$ ). One specimen (V18642.162) is relatively well preserved, and the others (V18642.163–164) are somewhat broken. The unciform is an irregular polygon and its height is greater than the width. There are two articular facets in proximal view. One is fan shaped and connected to the cuneiform, while the other with lunar is irregular quadrilateral. In the distal view, four articular facets are connected together to form an arcuate surface which is respectively linked to the magnum, Mc III, Mc IV and a degraded Mc V. The degree of development of hamulus is similar to that of living *Rhinoceros*.

#### Metacarpals

Metacarpal II ( $n = 1$ ). The proximal end is fragment. The diaphysis is straight. The distal articular facet is composed of the dome round surface and sesamoid surface. The concave in the lateral side (20 mm in width) is wider and deeper than that in the medial side (18 mm in width).

Metacarpal III ( $n = 1$ ). The proximal bone part was missing. The bone shaft is straight, and its cross section is flat oval in shape. The two articular facets connecting in palmar and articular facets for sesamoids are roughly equal in width (22 mm). The median part of bone shaft is 46.7 mm wide and 21.7 mm thick. The distal part is 55.5 mm wide and 26.6 mm thick.

Metacarpal IV ( $n = 2$ ). One specimen (V18642.166) is completely preserved, and the other (V18642.167) is somewhat broken in the distal part. The bone shaft is slightly curved to the distal-medial side. The cross section of proximal part is nearly triangular and the cross section of median and distal part is oval in shape. The proximal articular facet is oblate-triangular. In the proximal medial side, two articular facets are present in connection with Mc III. The large one is slim-oval in shape and 30 mm long, and small one is only somewhat preserved. In the proximal dorsal side, there are two grooves attaching to the ligament.

#### Sesamoids ( $n = 5$ )

All the specimens are well preserved. The articular facet of one specimen (V18642.152, which is connect

to Mc II) is trapezoidal with 27 mm long and 16 mm wide. The articular facets of another two specimens (V18642.153–154, which is connect to Mc IV) are oval in shape with size of  $29 \times 15$  and  $25 \times 14$  mm, respectively. The other two specimens (V18642.155–156, which is connect to Mc III) are more elongate. Their articular facets are  $36 \times 16$  and  $39 \times 12$  mm in size, respectively.

#### Phalanges

PhI of middle digit ( $n = 1$ ). The proximal prominence is obvious in the plantar/palmar side though the proximal articular facet is missing. The distal articular facet connecting PhII is slightly convex and extends to the dorsal and plantar/palmar sides.

PhII of middle digit ( $n = 3$ ). Two specimens (V18642.168–169) are well preserved, and the other (V18642.170) is somewhat broken in distal part. The bone shaft is short, wide and rectangular in outline. The proximal articular facet is oval, and the dorsal side is higher than the plantar side in lateral view. The distal articular facet is round and extends to the dorsal and plantar/palmar sides. The proximal prominence is present to attach the ligament.

PhIII of middle digit ( $n = 2$ ). The bone shaft is flat spade-shaped and the width is greater than the height. The proximal articular facet is oval in outline and 51 mm in width and 20 mm in height.

PhI of lateral digit ( $n = 4$ ). Four specimens are well preserved (V18642.173–176). The proximal articular facets are approximately square shaped and obviously concave at the centre. The distal articular facet and bone shaft form an acute angle. There are no median groove and proximal prominence.

#### Tarsals

Calcaneus ( $n = 1$ ). The proximal part is well preserved, and the distal part is partially preserved. There are three articular facets to contact calcaneus and astragalus, lateral astragalus facet, sustentacular facet and distal astragalus

Table 4. Metrical data and comparison of unciform of *Rhinoceros fusuiensis* (V18642.162) from YCF and extant Southeast Asian rhinos (mm).

	<i>Rhinoceros fusuiensis</i>	<i>Rhinoceros sondaicus</i> <sup>a</sup>	<i>Rhinoceros unicornis</i> <sup>a</sup>	<i>Dicerorhinus sumatrensis</i> <sup>a</sup>
L abs.	86	83–92 (87.6)	97.5–112 (105.2)	65.5–78 (70.6)
L anat.	65	65–74.5 (68.9)	75.5–86.5 (79.5)	48–63 (52)
W	66	60–74 (69)	74.5–82.5 (78.4)	52–61.5 (57.4)
H	51	47.5–55(52)	51.5–59(56.1)	41–50.5 (46.9)

Notes: L abs., absolute length, the largest dimensions of the bone measured from the foremost point of the facet for the semilunar to the most caudal point of the posterior apophysis; L anat., anatomical length, the distance from a plane tangent to the front surface to the posterior of the most caudal apophysis; W, width, taken tangent to the distal edge of the anterior surface; H, height, taken perpendicular to the width.

<sup>a</sup>Guérin (1980).

facet. The lateral astragalus facet is composed of relatively large and convex anterior surface and relatively small and concave posterior surface, two of which form an obtuse angle. The sustentacular facet is relatively smooth and smaller than the lateral astragalus facet on size. There is a shallow groove between lateral astragalus facet and sustentacular facet. The calcaneal tuberosity is slender. The medial process of the calcaneal tuberosity is slightly inflated.

*Metatarsals*

Mt II ( $n = 2$ ). The bone shaft is slender and the shape of its cross section changes from triangle on the proximal part to ellipse on the distal part. The proximal articular facet connecting the cuneiform is saddle shaped. On the lateral side, the proximal articular facets composed of the upper part to link external cuneiform and the lower part to attach Mt III.

Mt IV ( $n = 2$ ). The bone shaft is more robust than that of Mt II. In the proximal medial side, there are two articular facets to attach Mt III.

*Comparison and comments*

Yan, Wang, et al. (2014) have described the rhino dental remains from YCF as a new species, *Rhinoceros fusuiensis*. The present study intends to provide a detailed morphological study of the additional rhino postcranial skeleton fossils also from YCF. Most of postcranial bones of *Rhinoceros fusuiensis* from YCF, except calcaneus, are not significantly different from those of living Asian *Rhinoceros* on morphology, though a relatively smaller size is present on YCF *Rhinoceros*.

Although abundant Pleistocene rhino teeth fossils have been found in southern China, there are very few rhino postcranial remains reported besides YC (Colbert and Hooijer 1953). Due to the scarcity of comparative data on rhino postcranial fossils in China, especially the metacarpals and metatarsals, the extant Asian rhinos and *Rhinoceros sondaicus* fossils from Java combined with *Rhinoceros fusuiensis* from YCF are involved in the present study. The results (Figures 7 and 8) show that there is a clear distinction between the living *Rhinoceros* and *Dicerorhinus*. Furthermore, two species of extant

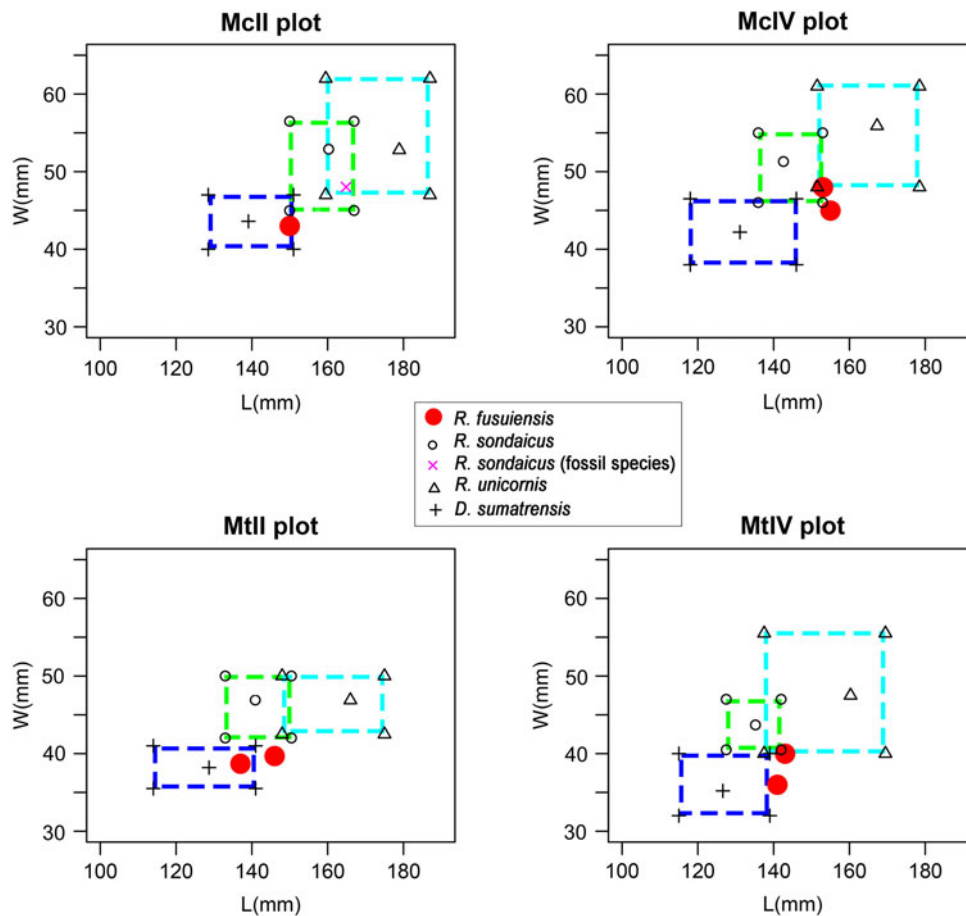


Figure 7. (Colour online) Metrical comparison of the width and length of Mcs and Mts of *Rhinoceros fusuiensis* from Yanliang Cave (red points) and the extant Southeast Asian rhinos (rectangles, each separate symbol on behalf of their means, data from Guérin [1980]; plus data of the *Rhinoceros sondaicus* fossils from Hooijer [1946]).

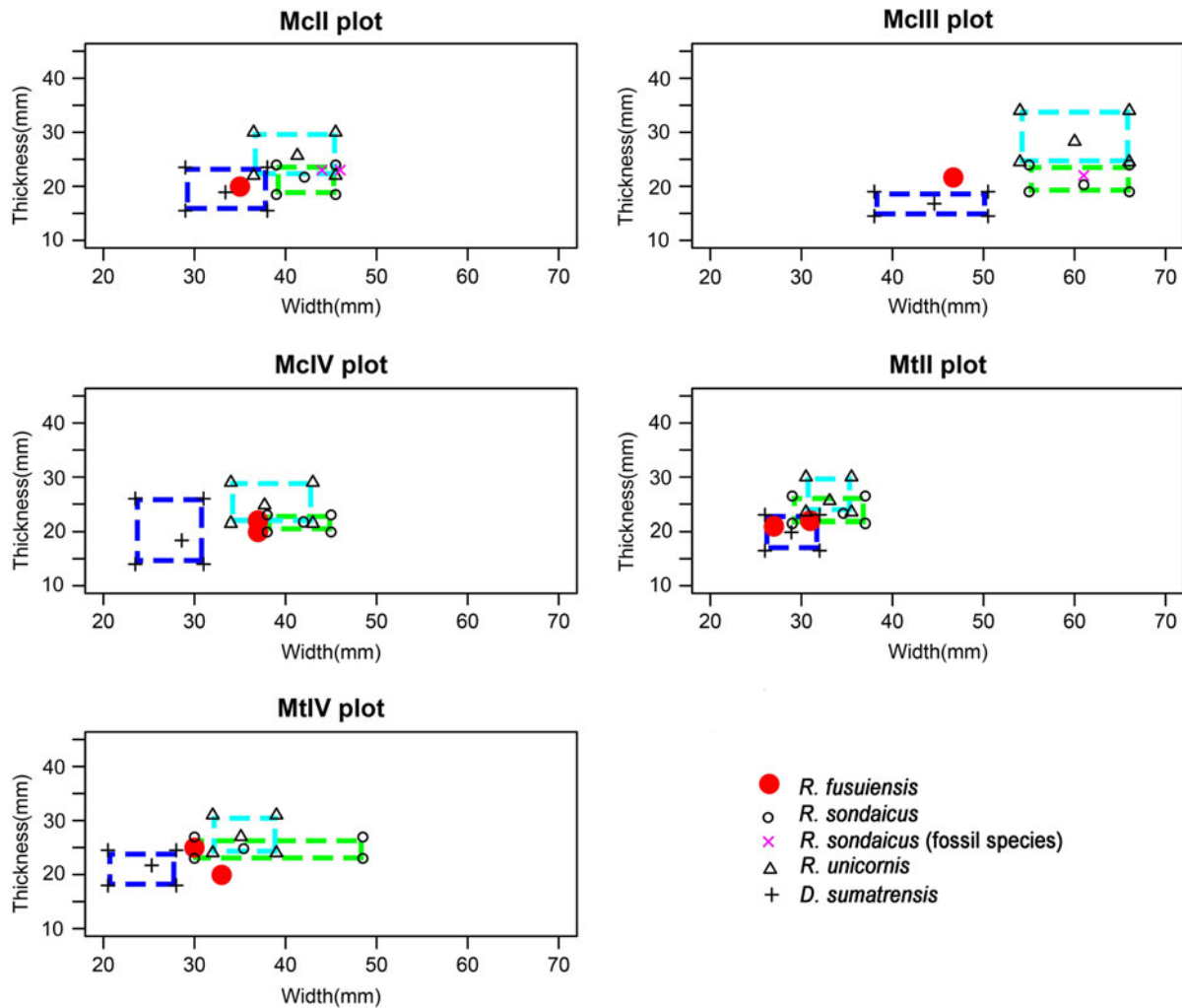


Figure 8. (Colour online) Metrical comparison of thickness and width of Mcs and Mts of *Rhinoceros fusuiensis* from Yanliang Cave (red points) and the extant Southeast Asian rhinos (rectangles, each separate symbol on behalf of their means, data from Guérin [1980]; plus data of the *Rhinoceros sondaicus* fossils from Hooijer [1946]).

*Rhinoceros* have no overlap on some indexes of measurements (e.g. the length and distal width of Mc IV and Mt II) or a few overlaps (e.g. the length and distal width of Mc II and Mt IV and the width and thickness of medial part of Mc IV and Mt IV). So, the quantitative indexes of measurements on metacarpus and metatarsus used in this study can provide available evidence on identifying rhino fossils. Based on the results shown in Figures 7 and 8, the sizes of metacarpus and metatarsus of *Rhinoceros fusuiensis* are smaller than those of the living *Rhinoceros* (*Rhinoceros unicornis* and *Rhinoceros sondaicus*), but greater than those of *Dicerorhinus sumatrensis*. Moreover, the measurements of *Rhinoceros fusuiensis* basically fall within the critical regions between extant *Rhinoceros* and *Dicerorhinus*, instead of any range of extant *Rhinoceros* species, which is possibly due to the primitive evolutionary level of *Rhinoceros fusuiensis*.

Although it is difficult to distinguish the Asian rhino species merely on the morphology of postcranial skeleton, their difference of calcaneus is still obvious as follows (Guérin 1980): the size, the proportion of distal astragalus facet and cubiod facet, the angle formed by sustentacular facet and astragalus axis, and so on. Especially, the calcaneus of *Rhinoceros fusuiensis* differs from other Asian rhino species in following aspects: (1) the measurements of *Rhinoceros fusuiensis* are less than those of two living *Rhinoceros* and extinct *Rhinoceros sinensis*, and more close to those of *Dicerorhinus* (Table 5); (2) the angle formed by the sustentacular facet and astragalus axis in *Rhinoceros fusuiensis* is almost orthogonal, which is larger than that in *Rhinoceros sondaicus* and more close to that in *Rhinoceros unicornis* (Figure 6) and (3) the medial process of the calcaneal tuberosity is only slightly inflated in *Rhinoceros fusuiensis*, which is more inflated in two living Asian

Table 5. Metrical data and comparison of calcaneus of *Rhinoceros fusuiensis* (V18642.178) from YCF and extant Southeast Asian rhinos (mm).

	<i>Rhinoceros fusuiensis</i>	<i>Rhinoceros sinensis</i> <sup>a</sup>	<i>Rhinoceros sondaicus</i> <sup>b</sup>	<i>Rhinoceros unicornis</i> <sup>b</sup>	<i>Dicerorhinus sumatrensis</i> <sup>b</sup>
H	100	132	119–138 (128.4)	136.5–160 (145.8)	95–117.5 (103.4)
DAT post. tal.	51		67.5–74.5 (70.9)	80.5–92 (84.3)	52–62 (56)
DT sust.	57	67	73–88.5 (82)	74–91 (83.7)	58–71 (65.3)
DT sommet.	34	65	45.5–55 (50.4)	59–72.5 (64.6)	35–46 (42.6)
DT mini. post.	27		28–35 (31.6)	39–41 (40)	22.5–31 (27.4)

Notes: H, height or length, taken parallel to the vertical axis of the bone; DAT post.tal., anterior–posterior diameter at lateral of posterior talar facet; DT sust., maximum transverse diameter distal epiphysis at sustentaculum tali; DT sommet., anterior–posterior diameter of the tuberosity; DT mini. post., minimum transverse diameter of the posterior edge.

<sup>a</sup>Jin and Liu (2009).

<sup>b</sup>Guérin (1980).

*Rhinoceros* species (Figure 6). The less developed medial process of the calcaneal tuberosity and the slightly inflated sustentacular tali of YCF specimens imply that *Rhinoceros fusuiensis* possible has a weak motility than that of living Asian *Rhinoceros*.

The calcaneus remains have been recovered from the Early Pleistocene RCF (Jin and Liu 2009) and the Middle Pleistocene GCQ (Pei et al. 1965; Li and Wen 1986). Compared to the calcaneus from these two sites, calcaneus of *Rhinoceros fusuiensis* is relatively small and slender, bears a narrow distance between the lateral astragalus facet and sustentacular facet, and has a weak inflation of the medial process of the calcaneal tuberosity.

## Discussion

In sum, the new Perissodactyl specimens recovered from YCF include *Hesperotherium sinense*, *Tapirus sanyuanensis* and *Rhinoceros fusuiensis*.

The genus *Hesperotherium* is one kind of Neogene relic taxa. There have been more than 10 localities with *Hesperotherium sinensis* remains which are all dated to be the Early Pleistocene (Teilhard de Chardin and Piveteau 1930; Li et al. 1978; Tang et al. 1983; Huang and Fang 1991; Qiu 2002; Li and Deng 2003; Qiu et al. 2004; Zheng 2004; Tong 2006; Jin and Liu 2009; Zhao and Zhang 2013; Jin et al. 2014; Wang, Liao, et al. 2014). Tong (2006) divided the Quaternary *Hesperotherium* into two types. The YCF specimen is most similar to those from LGC and MCT and should belong to the primitive type because of its small size and the degenerate trace of hypoconulid on m3.

*Tapirus sanyuanensis* was established by Huang and Fang (1991) based on the tapir fossils from LCW. It is considered as a transitional species from *Tapirus yunnanensis* to *Tapirus sinensis*. At present, all localities with *Tapirus sanyuanensis* are dated as the Middle to Early Pleistocene, such as RCF, LCJ, BCL, MCT, BCB and HQH (Tong and Xu 2001; Tong et al. 2002; Zheng 2004; Jin and Liu 2009; Zhao and Zhang 2013; Jin et al. 2014; Wang, Liao, et al. 2014). The YCF specimens are more

closely related to those from RCF and LCW by having a small overall size and the primitive dental morphology.

*Rhinoceros fusuiensis* was recently erected by Yan, Wang et al. (2014) based on the dental specimens from YCF, also including the rhino remains from LCW, MCT and Pauk, Myanmar (Huang and Fang 1991; Zin-Maung-Maung-Thein et al. 2010; Wang, Liao, et al. 2014). With its small size, lower crown and other primitive dental characteristics, *Rhinoceros fusuiensis* is considered to be the most primitive *Rhinoceros* species during Quaternary in southern China, corresponding to the age of early Early Pleistocene (1.8–2.6 Ma).

Compared with the other Early Pleistocene *Gigantopithecus* fauna sites in southern China, the YCF fauna is most close to that of LCW (Huang and Fang 1991), MCT (Wang, Liao, et al. 2014) and BCL (Jin et al. 2014). BCL is located in the same area as YCF and has been dated as 2.0 Ma by palaeomagnetic evidence (Sun et al. 2014). The systematic analysis on carnivore fossils also demonstrate that the age of YCF should be the early Early Pleistocene (Zhu et al. 2014, 2015).

As the typical forest-type animal, *Hesperotherium* was sensitive to the change of environment and lived in a warm and humid forest (Chen 2008). *Tapirus* generally lives in a semi-aquatic environment and also adapts to a warm and humid tropical forest (Tong and Xu 2001). Fortelius (1982) thought that the distinction between brachyodont and hypsodont rhino teeth has certain correlations with their food within the living environment. Based on this view, Xu (1986) divided the Quaternary rhino teeth into three types: browsing, grinding and transitional types. *Rhinoceros fusuiensis* resembles *Rhinoceros sondaicus* in the following dental characters. On the upper cheek teeth, the buccal side is higher than lingual side on the occlusal surface, the ectoloph wear profile is wavy-shaped and the secondary folds are not developed. Therefore, both of them should belong to the browsing type. The extant *Rhinoceros sondaicus* normally survives in the dense forest and low-lying areas with waters and mud nearby (Groves 1967; Groves and Leslie 2011). In a word, the Perissodactyl

fossils indicate that the YCF fauna lived in a humid and warm tropical forest with waters and mud nearby. This environment was favourable for habitation of high-evolved primates such as *Giantopithecus blacki*.

## Conclusion

The new Perissodactyl remains associated with *Giantopithecus blacki* recovered from Yanliang Cave during the excavations in 2011 have been identified as *Hesperotherium sinense*, *Tapirus sanyuanensis* and *Rhinoceros fusuiensis*, which are the common elements of the Early Pleistocene *Giantopithecus*–*Sinomastodon* fauna (Wang, Jin, et al. 2014). The Perissodactyl assemblage from Yanliang Cave is most similar to those from Longgupo Cave (Chongqing) and Mohui Cave (Guangxi), indicating its age as the early Early Pleistocene (~2.0 Ma). These Perissodactyl fossils also imply a tropical bushy and forested environment with a humid and warm climate favourable for habitation of high-evolved primates such as *Giantopithecus blacki*.

## Acknowledgements

Dr Yuki Tomida is specially thanked for the continuous support, encouragement and discussions on palaeontological research. We also thank Dr Yuri Kimura for inviting us for this contribution. We are grateful for the discussions and field assistance from Haowen Tong, Jim I. Mead, Guangbiao Wei, Wei Wang, Jiajian Zheng, Qinqi Xu, Yingqi Zhang, Zhilu Tang, Yihong Liu, Qiuyuan Wang and Weimin Zheng. We appreciate very much the hardwork of Dr Gareth Dyke for expediting the process of this manuscript. We are also grateful to the anonymous reviewers who have spent time providing the instructive comments to improve this manuscript.

## Disclosure statement

No potential conflict of interest was reported by the authors.

## Funding

This work was supported by the Program of Chinese Academy of Sciences [grant number KZZD-EW-03], National Natural Science Foundation of China [grant number 41202017] and the State Key Laboratory of Palaeobiology and Stratigraphy (Nanjing Institute of Geology and Palaeontology, CAS) [grant number 143109].

## References

Chen SK. 2008. A review on Chinese Neogene Chalicotheres. In: Dong W, editor. Proceedings of the Eleventh Annual Meeting of the Chinese Society of Vertebrate Paleontology. Beijing: China Ocean Press. [in Chinese with English abstract] p. 31–41.

Colbert H, Hooijer A. 1953. Pleistocene mammals from the limestone fissures of Szechwan, China. *Bull Am Mus Nat Hist*. 102(1):1–134.

Coombs MC. 1978. Additional *Schizotherium* material from China, and a review of *Schizotherium* dentitions (Perissodactyla, Chalicotheriidae). *Am Mus Novit*. 2647:1–18.

Dong W, Jin CZ, Wang Y, Xu QQ, Qin DG, Sun CK, Zhang LM. 2013. New materials of Early Pleistocene *Sus* from Sanhe Cave, Chongzuo, Guangxi, South China. *Acta Anthropol Sin*. 32:63–76. [in Chinese with English abstract].

Dong W, Liu JY, Zhang LM, Xu QQ. 2014. The early pleistocene water buffalo associated with *Giantopithecus* from Chongzuo in southern China. *Quat Int*. 354:86–93. doi:10.1016/j.quaint.2013.12.054.

Dong W, Pan WS, Sun CK, Xu QQ, Qin DG, Wang Y. 2011. Early Pleistocene ruminants from Sanhe Cave, Chongzuo, Guangxi, South China. *Acta Anthropol Sin*. 30:192–205. [in Chinese with English abstract].

Fortelius M. 1982. Ecological aspects of dental functional morphology in the Plio-Pleistocene Rhinoceros of Europe. In: Kurtén B, editor. Teeth, form, and evolution. New York, NY: Columbia University Press; p. 163–181.

Groves CP. 1967. On the rhinoceros of Southeast Asia. *Saugetierkundliche Mitteilungen*. 15:221–237.

Groves CP, Leslie DM. 2011. *Rhinoceros sondaicus* (Perissodactyla: Rhinocerotidae). *Mamm Spec*. 43(887):190–208. doi:10.1644/887.1.

Guérin C. 1980. Les rhinoceros (Mammalia, Perissodactyla) du Miocène terminal au Pléistocène supérieur en Europe occidentale [The rhinoceros (Mammalia, Perissodactyla) from Miocene to Pleistocene in Western Europe]. *Documents Laboratoire Géologie Lyon*. 79(1–3):1–1185. [in French].

Harrison T, Jin CZ, Zhang YQ, Wang Y, Zhu M. 2014. Fossil *Pongo* from the Early Pleistocene *Giantopithecus* faunas of Chongzuo, Guangxi, southern China. *Quat Int*. 354:59–67. doi:10.1016/j.quaint.2014.01.013.

Hooijer DA. 1946. Prehistoric and fossil rhinoceroses from the Malay Archipelago and India. *Leiden Zool Meded*. 26:1–138.

Hooijer DA. 1947. On fossil and prehistoric remains of *Tapirus* from Java, Sumatra and China. *Leiden Zool Meded*. 27:253–299.

Huang WB, Fang QR. 1991. Wushan Hominid site. Beijing. [in Chinese with English summary] Ocean Press.

Jin CZ, Liu JY. 2009. Paleolithic site – the Renzidong Cave, Fanchang, Anhui, China. Beijing. [in Chinese with English summary] Science Press.

Jin CZ, Pan WS, Zhang YQ, Cai YJ, Xu QQ, Tang ZL, Wang W, Wang Y, Liu JY, Qin DG, et al. 2009. The *Homo sapiens* Cave hominin site of Mulan Mountain, Jiangzhou District, Chongzuo, Guangxi with emphasis on its age. *Chin Sci Bull*. 54(21):3848–3856. doi:10.1007/s11434-009-0641-1.

Jin CZ, Qin DG, Pan WS, Tang ZL, Liu JY, Wang Y, Deng CL, Zhang YQ, Dong W, Tong HW, 2009. A newly discovered *Giantopithecus* fauna from Sanhe Cave, Chongzuo, Guangxi, South China. *Chin Sci Bull*. 54(5):788–797. doi:10.1007/s11434-008-0531-y.

Jin CZ, Qin DG, Pan WS, Wang Y, Zhang YQ, Deng CL, Zheng JJ. 2008. Micromammals of the *Giantopithecus* fauna from Sanhe Cave, Chongzuo, Guangxi. *Quat Sci*. 28:1129–1137. [in Chinese with English abstract].

Jin CZ, Tomida Y, Wang Y, Zhang YQ. 2010. First discovery of fossil *Nesolagus* (Leporidae, Lagomorpha) from Southeast Asia. *Sci China Ser D*. 53(8):1134–1140. doi:10.1007/s11430-010-4010-3.

Jin CZ, Wang Y, Deng CL, Harrison T, Qin DG, Pan WS, Zhang YQ, Zhu M, Yan YL. 2014. Chronological sequence of the early Pleistocene *Giantopithecus* faunas from cave sites in the Chongzuo, Zuojiang River area, South China. *Quat Int*. 354:4–14. doi:10.1016/j.quaint.2013.12.051.

Koken E. 1885. Über fossile Saugethiere aus China [The animal fossil from China]. *Paläontologische Abhandlungen*. 3(2):31–114. [in German].

Li XC, Deng K. 2003. Early Pleistocene Chalicotheres fossils from Huangjiawan, Zhen an, Shaanxi, China. *Vert Palasiat*. 41(4):332–336. [in Chinese with English abstract].

Li YP, Pan YR, Lu QW. 1978. The Early Pleistocene mammalian fauna from Yuanmou, Yunnan Province, China. In: Institute of Vertebrate Paleontology and Paleoanthropology, Chinese Academy of Science editors. Beijing. [in Chinese] Science Press; p. 101–120.

- Li YX, Wen BH. 1986. Guanyindong – a lower Paleolithic site at Qianxi County, Guizhou Province. Beijing. [Chinese with English summary] Cultural Relics Press.
- Liu W, Jin CZ, Zhang YQ, Cai YJ, Xing S, Wu XJ, Cheng H, Edwards RL, Pan WS, Qin DG, et al. 2010. Human remains from Zhirendong, South China, and modern human emergence in East Asia. *Proc Natl Acad Sci.* 107(45):19201–19206. doi:10.1073/pnas.1014386107.
- Mead JI, Moscato D, Wang Y, Jin C, Yan Y, Mead JI, Moscato D, Jin CZ, Wang Y. 2014. Pleistocene *lizards* (Squamata, Reptilia) from the karst caves in Chongzuo, Guangxi, southern China. *Quat Int.* 354: 94–99. doi:10.1016/j.quaint.2014.03.047.
- Owen R. 1870. On fossil remains of mammals found in China. *Quat J Geol Soc.* 26(1–2):417–439.
- Pei WZ, Yuan ZX, Lin YP, Zhang YY. 1965. Discovery of Palaeolithic cheat artifacts 617 in Kuan-Yin-Tung Cave in Chien-His-Hsien of Kueichow Province. *Vert PalAsiat.* 9(3): 270–279. [in Chinese with English summary].
- Qiu ZX. 2002. *Hesperotherium* – a new genus of the last Chalicotheres. *Vert PalAsiat.* 40(4):317–325. [in Chinese with English abstract].
- Qiu ZX, Deng T, Wang BY. 2004. Early Pleistocene mammalian fauna from Longdan, Dongxiang, Gansu, China. *Palaentol Sin.* 27:1–198. Whole number 191, new series C, Number 27. [in Chinese with English summary].
- Qiu ZX, Wang BY. 2007. Paraceratheres fossils of China. Beijing: Science Press. [in Chinese with English summary].
- Sun L, Wang Y, Liu CC, Zuo TW, Ge JY, Zhu M, Jin CZ, Deng CL, Zhu RX. 2014. Magnetochronological sequence of the Early Pleistocene *Gigantopithecus* faunas in Chongzuo, Guangxi, southern China. *Quat Int.* 354:15–23. doi:10.1016/j.quaint.2013.08.049.
- Takai M, Zhang YQ, Kono RT, Jin CZ. 2014. Changes in the composition of the Pleistocene primate fauna in southern China. *Quat Int.* 354: 75–85. doi:10.1016/j.quaint.2014.02.021.
- Tang YJ, Zong GF, Xu QQ. 1983. Mammalian fossils and stratigraphy of Linyi, Shanxi. *Vert PalAsiat.* 21(1):77–86. [in Chinese with English abstract].
- Teilhard de Chardin P, Piveteau J. 1930. Les mammifères fossiles de Nihowan (Chine) [The mammalian fossils from Nihewan (China)]. *Ann Paleontol.* 19:1–134. [in French].
- Tong HW. 2005. Dental characters of the Quaternary tapirs in China, their significance in classification and phylogenetic assessment. *Geobios.* 38(1):139–150. doi:10.1016/j.geobios.2003.07.006.
- Tong HW. 2006. *Hesperotherium sinensis* – a Chalicotheres (Perissodactyla, Mammalia) from the Early Pleistocene Liucheng *Gigantopithecus* Cave. *Vert PalAsiat.* 44(4):347–365. [in Chinese with English abstract].
- Tong HW, Liu JY, Han LG. 2002. On fossil remains of Early Pleistocene tapir (Perissodactyla, Mammalia) from Fanchang, Anhui. *Chin Sci Bull.* 47(7):586–590. doi:10.1360/02tb9135.
- Tong HW, Xu F. 2001. On the origin and evolution of Quaternary Tapirs in China. In: Deng T, Wang Y, editors. *Proceedings of the Eighth Annual Meeting of the Chinese Society of Vertebrate Paleontology.* Beijing. [in Chinese with English abstract] China Ocean Press; p. 133–141.
- Wang W, Liao W, Li DW, Tian F. 2014. Early Pleistocene large-mammal fauna associated with *Gigantopithecus* at Mohui Cave, Bubing Basin, South China. *Quat Int.* 354:122–130. doi:10.1016/j.quaint.2014.06.036.
- Wang Y, Jin CZ, Mead JI. 2014. New remains of *Sinomastodon yangziensis* (Proboscidea, Gomphotheriidae) from Sanhe karst cave, with discussion on the evolution of Pleistocene *Sinomastodon* in South China. *Quat Int.* 339–340:90–96. doi:10.1016/j.quaint.2013.03.006.
- Wang Y, Jin CZ, Zhang YQ, Qin DG. 2010. Murid rodents from the *Homo sapiens* Cave of Mulan Mountain, Chongzuo, Guangxi, South China. *Acta Anthropol Sin.* 29:303–316. [in Chinese with English abstract].
- Wang Y, Qin DG, Jin CZ, Pan WS, Zhang YQ, Zheng JJ. 2009. Murid rodents of the new discovered fauna from the Sanhe Cave, Chongzuo, Guangxi, South China. *Acta Anthropol Sin.* 28:73–87. [in Chinese with English abstract].
- Xu XF. 1986. *Dicerorhinus Kirchibergensis* (Jäger, 1839) from the late middle Pleistocene mammalian fauna of Anping, Liaoning. *Vert PalAsiat.* 24(3):229–242. [in Chinese with English abstract].
- Yan YL, Jin CZ, Zhu M, Liu YH, Liu JY. 2014. Age profile of *Rhinoceros* from the Yanliang Cave, Fusui County, Guangxi, South China. *Acta Anthropol Sin.* 33(4):534–544. [in Chinese with English abstract].
- Yan YL, Wang Y, Jin CZ, Mead JI. 2014. New remains of *Rhinoceros* (Rhinocerotidae, Perissodactyla, Mammalia) associated with *Gigantopithecus blacki* from the Early Pleistocene Yanliang Cave, Fusui, South China. *Quat Int.* 354:110–121. doi:10.1016/j.quaint.2014.01.004.
- Zhang YQ, Jin CZ, Cai YJ, Kono R, Wang W, Wang Y, Zhu M, Yan YL. 2014. New 400–320 ka *Gigantopithecus blacki* remains from Hejiang Cave, Chongzuo City, Guangxi, South China. *Quat Int.* 354: 35–45. doi:10.1016/j.quaint.2013.12.008.
- Zhang YQ, Jin CZ, Takai M. 2010. A partial skeleton of *Macaca* (Mammalia, Primates) from the Early Pleistocene Queque Cave site, Chongzuo, Guangxi, South China. *Vert PalAsiat.* 48:275–280.
- Zhao LX, Jin CZ, Qin DG, Pan WS. 2008. Description of new fossil teeth of *Gigantopithecus blacki* from Sanhe Cave, Chongzuo, Guangxi Southern China with comments on evolutionary trends in *Gigantopithecus* dental size. *Quat Sci.* 28:1139–1144. [in Chinese with English abstract].
- Zhao LX, Zhang LZ. 2013. New fossil evidence and diet analysis of *Gigantopithecus blacki* and its distribution and extinction in South China. *Quat Int.* 286:69–74. doi:10.1016/j.quaint.2011.12.016.
- Zheng SH. 2004. Jianshi Hominid site. Beijing: Science Press. [in Chinese with English summary].
- Zhu M, Schubert BW, Liu JY, Wallace SC. 2014. A new record of the saber-toothed cat *Megantereon* (Felidae, Machairodontinae) from an Early Pleistocene *Gigantopithecus* fauna, Yanliang Cave, Fusui, Guangxi, South China. *Quat Int.* 354:100–109. doi:10.1016/j.quaint.2014.06.052.
- Zhu M, Yan YL, Liu YH, Tang ZL, Qin DG, Jin CZ. 2015. The new Carnivore remains from the Early Pleistocene Yanliang *Gigantopithecus* fauna, Guangxi, South China. *Quat Int.* [on line] doi:10.1016/j.quaint.2015.01.009.
- Zin-Maung-Maung-Thein, Takai M, Takehisa T, Egi N, Thang-Htike, Nishimura T, Maung-Maung Zaw-Win. 2010. A review of fossil *Rhinoceros* from the Neogene of Myanmar with description of new specimens from the Irrawaddy sediments. *J Asian Earth Sci.* 37(2): 154–165.

Copyright of Historical Biology is the property of Taylor & Francis Ltd and its content may not be copied or emailed to multiple sites or posted to a listserv without the copyright holder's express written permission. However, users may print, download, or email articles for individual use.